JOWRM

Journal of Water Resources Management

Journal homepage: https://journal.water.gov.my

e-ISSN: 2811-3578

Experimental Analysis of Ideal Hydraulic Pressure for Sediment Movement in Closed Pipe Flow

Muh. Syafa'at S.Kuba[1,a*], Muhammad Saleh Pallu[1,b], Bambang Bakri[1,c]

[1]Department of Civil Engineering, Universitas Hasanuddin

Corresponding Author; Syafaat_skuba@unismuh.ac.id

Email: [a] Syafaat_skuba@unismuh.ac.id, [b] salehpallu@gmail.com, [c] bambangbakri@gmail.com

Received 15 June 2026;
Accepted 16 Oct 2026;
Available online 21 Oct 2026

Abstract: Sediment transport in closed pipe systems plays a crucial role in the efficiency and sustainability of water distribution, drainage, and sewage infrastructure. Deposition of particles in pipelines can increase head loss, reduce hydraulic performance, and accelerate system deterioration. This study presents a laboratory-scale experimental investigation to analyze the movement of sediments under controlled flow conditions in closed circular pipes. Key hydraulic and sediment parameters such as flow velocity, concentration, and particle size—were examined, and the analysis was supported by dimensionless parameters such as the Reynolds number, Froude number, and Shields parameter. Experimental results identified three flow regimes: non-deposition, incipient deposition, and full deposition. The findings quantitatively demonstrate that self-cleansing conditions were sustained under fully turbulent flow, with Reynolds numbers ranging from 2.40×10^4 to 4.18×10^4, Froude numbers from 0.61 to 1.07, bed shear stress from 0.577 to 1.552 Pa, and Shields parameter values from 0.071 to 0.191. These results indicate that velocity-induced shear stress exceeding the critical threshold for incipient sediment motion can maintain sediment mobility and prevent deposition in pressurized closed pipe systems. The study therefore contributes to a more rigorous understanding of sediment behavior in closed conduits and provides a quantitative reference for the design, operation, and maintenance of water distribution, drainage, and sewage networks to minimize clogging, control head loss, and ensure long-term hydraulic reliability.

Keywords: Sediment transport, Closed pipe flow, Ideal hydraulic pressure, Dimensionless parameters, Reynolds number, Shields parameter, Experimental hydraulics.

1. Introduction

The movement of sediment in closed piping systems represents a critical challenge in hydraulic engineering, particularly within drainage networks, drinking water supply lines, and sewage transportation systems (Taiwo et al., 2025). Sediment transported by the flow often undergoes deposition at specific points in the pipeline, which can degrade hydraulic efficiency, increase energy consumption, and accelerate structural deterioration. Therefore, a clear understanding of sediment transport mechanisms in closed conduits is essential for the sustainable planning and maintenance of pipeline infrastructure (Safari & Rahimzadeh Arashloo, 2023).

Sediment transport in closed pipes is highly complex because of the simultaneous interaction between solid particles and turbulent fluid motion within confined geometries. Laboratory investigations have demonstrated that physical factors such as flow velocity, sediment concentration, particle size, and pipe geometry strongly influence transport efficiency and deposition patterns (Liu et al., 2022). Complementary large-scale experiments further confirm that even minor variations in hydraulic conditions can significantly alter deposition rates (Naves et al., 2020).

Recent studies also highlight the role of flow regimes whether unimodal or bimodal in shaping transportation efficiency and energy demand in pipeline systems (Gooran et al., 2025). Laboratory-scale testing thus becomes indispensable, not only for revealing the dynamics of fluid–particle mixtures but also for validating emerging numerical and artificial intelligence (AI)-based predictive approaches (Montes et al., 2020).

In the field of modeling, advanced computational techniques such as Random Forest, genetic algorithms, and evolutionary polynomial regression have shown promise in improving predictive accuracy of sediment transport in closed systems (Kargar et al., 2021). Similarly, Sha et al. (2025) evaluated turbulence models for two-phase flows, a condition frequently encountered in sediment-laden pipelines. These approaches contribute to a better understanding of complex flow dynamics under pressurized conditions. On the geometric side, Yao et al. (2025) employed a two-phase Eulerian–Eulerian model to study sand transport in sloping pipes, while Wang et al. (2024) developed a two-layer model to capture density wave amplification and sublayer erosion. Together, these findings underscore the importance of integrating experimental and numerical methods for a

Corresponding Author: Syafaat_skuba@unismuh.ac.id
2026 JPS Publishing. All right reserved.

comprehensive understanding of sediment transport.

Given the complexity of the phenomenon and the practical importance of minimizing deposition, this study aims to consolidate experimental findings from laboratory-scale investigations of sediment transport in closed pipes. The primary objectives are fourfold:

1. To analyze the effect of pipe diameter variations on sedimentation levels.
2. To evaluate the relationship between flow velocity and sediment deposition tendencies.
3. To identify the influence of sediment grain size on deposition behavior.
4. To determine the relationship between dimensionless flow parameters (e.g., Reynolds and Froude numbers) and sedimentation patterns.

The novelty of this work lies in its systematic integration of small-scale laboratory experiments with hydraulic dimensionless analysis to identify critical velocity thresholds and deposition mechanisms. Unlike most previous research, which has focused predominantly on large-scale field studies or numerical simulations, this study provides empirical baseline data on the combined effects of pipe diameter, sediment size, and flow velocity. Furthermore, the experimental results are positioned as validation benchmarks for computational and AI-driven predictive models, thereby bridging traditional laboratory research with modern data-driven approaches. Ultimately, the contributions of this study hold both theoretical value and practical relevance for the design, operation, and maintenance of irrigation, drainage, and industrial piping systems

2. Literature Review

2.1 Sediment Transport

Sediment transport is defined as the process of moving solid particles carried by the flow of water through the mechanisms of erosion, entrainment, transportation, deposition, and resuspension (Montes et al., 2020). Sediment particles can be in the form of sand, silt, gravel, or organic material derived from soil erosion, surface runoff, or anthropogenic activity. In the context of hydraulics, sediment carried by flows is usually categorized into three main forms, namely bed load, suspended load and dissolved load.

The role of sediment transport in hydraulic systems is crucial because it directly affects hydraulic capacity, infrastructure lifespan, and water quality. In pipeline and conduit systems, sediment accumulation can increase hydraulic roughness, increase energy loss, and reduce flow capacity (Babar et al., 2025). This can cause clogging or stagnation, so the self-cleaning velocity parameter is an important consideration in the design of the piping system (Orang & Pouranfard, 2022).

In addition to the hydraulic aspect, sediment transportation also plays a role in water quality. Sediment serves as a carrier medium for various pollutants, including organic matter, heavy metals, and nutrients such as phosphorus (Chen et al., 2025). The sediment resuspension process at the time of sudden discharge changes can increase the concentration of pollutants in the water and worsen the condition of the receiving water body (Sha et al., 2025). This phenomenon is often observed in urban drainage systems and is known as the first flush effect, which is the sudden release of sediment and pollutants at the beginning of a rainy event.

2.2 Closed Channels

Pipes are closed channels that are generally circular cross-section and are used to flow fluids with a full flow cross-section. The fluid flowing through the pipeline can be either a liquid or a gaseous substance and the pressure can be greater or less than the atmospheric pressure. If the liquid in the pipeline is not full, the flow is included in the open channel flow or because the pressure in the pipeline is equal to the atmospheric pressure (the liquid in the pipeline is not full), the flow is included in the open flow (Jang et al., 2024).

2.2.1 Types of Closed Channels

Closed channels are conduits designed to transport fluids in a fully enclosed system, ensuring flow under pressure or gravity. Their classification, such as pipes, culverts, and siphons, is crucial for optimizing hydraulic efficiency and structural reliability.

A pipeline is a piping system used to flow fluids, both liquid and gas, from one location to another. Pipes usually have a circular cross-section and function to flow fluids with pressures that can be greater or smaller than atmospheric pressure (Zhang et al., 2023). In the context of water distribution, pipelines are essential to ensure the supply of clean water to consumers. A pipeline network that carries water from a source to consumers. The system can use gravity or pump methods to move the water (Luo et al., 2023). A closed channel used to drain fluid. Pipes can be made of various materials such as PVC, iron, or copper, depending on the application and the type of fluid being flowed.

A closed drainage channel is a drainage system designed to drain water, especially rainwater, from one area to another without being directly exposed to the outside environment (M. Casini, 2022). These channels are typically made of materials such as precast concrete, pipes, or other materials that can withstand the pressure and flow of water.

2.2.2 Pipe Flow

Flow in a pipeline is the phenomenon of the movement of fluids, both liquid and gas, through a pipeline. This flow can occur laminar or turbulent, depending on the flow speed and viscosity of the fluid. Factors such as pipe diameter, pipe surface roughness, and flow speed affect the type of flow that occurs in a pipe. The study of flows within pipes has many benefits and is important to understand it well (A. K. Coker, 2024). In addition, a good understanding of the flow within the pipeline can also be helpful in analyzing and troubleshooting issues related to the piping system, such as increased pressure, leaks, or temperature control.

2.3 Transport of sediment in pipes

Sediment transport in pipelines plays an important role, especially in the field of mud deposit removal and dredging. This system is used because it is able to move sedimentary materials with minimal energy loss without causing deposition that hinders hydraulic efficiency (Li et al., 2024). Therefore, the most crucial aspect is the ability to predict energy losses and determine the minimum speed or critical velocity to keep the pipeline free from material.

Slurry is a mixture of solids and liquids. A sludge deposit is a concentrated sludge or slurry that has a very fine amount of material that provides high viscosity. A typical example of slurry is a mixture of solid-liquid substances found in plant mineral processes and the dredging of material from rivers and weirs (Thorn et al., 2025). The ability of a fluid in horizontal

motion to suspend sedimentary particles depends on the equilibrium effect of the two forces (Sha et al., 2025).

In a heterogeneous flow, the particles are all in suspension but their vertical distribution is not uniform, with the concentration of the particles being greater in essence. This is the most economical regime for the transport of solids in pipelines, as is illustrated in Figure 1.

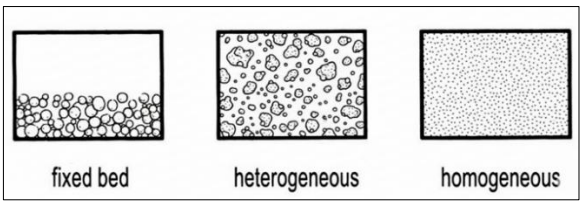

Fig.1 - Flow regime and distribution of sediment in pipes

Another particle property that has an influence in the classification of sediment flow regimes is specific gravity, as high specific gravity causes particles to settle. In addition to depending on the nature of the particles, the tendency to settle also depends on the flow speed and Reynold's number. The tendency to settle will decrease when the speed or Reynold's number is high.

3. Methodology

3.1 Data collection

This study uses a combination of data consisting of laboratory experiments on a laboratory-scale closed pipe system. The data used in this study include:

i. Rig configuration: closed pipe loop (transparent material for visualization) with 3 variations of inner diameter, effective measuring length ≥ 50 D to ensure the flow expands L.
ii. Working fluids & sediments: clean water and water sediment mixtures with controlled volume fractions; Measured grain size distribution to obtain and spectrum $C_v\ d_{50}\ d$.
iii. Instruments: flowmeter (discharge), manometer/pressure transducer (ΔP), thermometer (T) for viscosity & density, camera, sampling gravimetric $Q\mu\ (T)\ \rho(T)$.
iv. Operating variables: flow/speed(), head/inclination, pipe diameter, grain size, solids fraction, temperature. $Q,\ VD\ d_{50}\ C_vT$.
v. Main outcomes: sediment regime status critical velocity, energy penalty ($\Delta P/L$), and dimensionless parameters (Re, Fr,) $V_c\theta$.

Periodic calibration consists of a flowmeter, a pressure transducer that loads ≥3 repeats per operating point, and an uncertainty propagation (Gauss formula) for . Data quality criteria: CoV for and $\Delta P/L$; Visual inspection ensures steady flow $V, f, \tau_b, \theta < 5\%V$.

3.2 Reynolds Number

Reynolds numbers and their significance in determining flow regimes are crucial in predicting and analyzing fluid behavior in piping systems (Gong & Wang, 2024). This knowledge plays an important role in solving problems related to increased pressure, leakage, or temperature control in the system. In fluid flow, the force acting consists of the inertial force, which deals with the velocity and density of the fluid, and the viscosity force, which deals with the viscosity and length of the characteristics. Reynolds numbers quantify the ratio between inertial force (Fi) and viscosity force (Fv) (Monokrousos et al., 2024):

$$Re = \frac{F_i}{F_v} = \frac{\rho v^2 D}{\mu \frac{v}{D}} = \frac{\rho v D^2}{\mu} \quad (1)$$

The replacement of dynamic viscosity using kinematic viscosity ( ) equation 1 can be simplified tov $= \frac{\mu}{\rho}$ (2)

$$Re = \frac{vD}{\nu}$$

where Re is a Reynolds number representing the ratio *of Fi* to Fv; D is the diameter of the pipe (m); ν is the kinematic viscosity (m²/s); μ is the dynamic viscosity (Pa·s); and ρ is the fluid density (kg/m³).

By understanding the different types of flows and the factors that affect them, they can optimize the performance of existing piping systems, thereby improving operational efficiency and reducing the potential for system breakdowns or failures.

3.3 Bernoulli's Equation

The Bernoulli's equation is a fundamental concept in fluid dynamics that plays an important role in understanding pipeline flow in engineering systems. So it helps in analyzing the relationship between pressure, velocity, and elevation in fluid flow. By applying Bernoulli's equations, engineers can predict and optimize the behavior of fluids in pipelines, which is important for a wide range of engineering applications (Alkahtani et al., 2023).

The Bernoulli's reflects the principle of energy conservation, by equalizing the amount of kinetic energy, potential energy, and static pressure at two points along the pipeline. The Bernoulli's equation, which describes the relationship between pressure, velocity, and altitude in the flow of fluid through a pipe, is formulated as follows (García-Grimaldo & Campos-Cantón, 2023):

$$P_1 + \frac{1}{2}\rho v_1^2 + \rho g h_1 = P_2 + \frac{1}{2}\rho v_2^2 + \rho g h_2 \quad (3)$$

where P_1 and P_2 are the pressures at points 1 and 2 (Pa); ρ is the density of the fluid (kg/m³); v_1 and v_2 are the velocity at points 1 and 2 (m/s); g is the acceleration of gravity (m/s²); and h_1 and h_2 are the elevation above the reference point (m).

The diameter of the pipe has a significant impact on the flow speed of the fluid in it. The larger diameter allows a larger volume of liquid to flow (Aung et al., 2024). Fluids with higher viscosity will experience greater resistance to flow in the pipe. A smoother pipe wall will result in lower friction resistance and a higher flow rate, while a rougher pipe wall can lead to increased turbulence and energy loss (Ding et al., 2024).

3.4 Deposit Velocity

In the discussion of this velocity deposit, the estimate is detailed by proposing equations from Oskar and Turian. Oskar and Turian are said to have developed a semi-empirical correlation that can be used to calculate the value of deposition velocity (DV) (Lienhard et al., 2022). Illustration shown in the Figure 2.

Diterbitkan oleh JPS Publishing
https://journal.water.gov.my

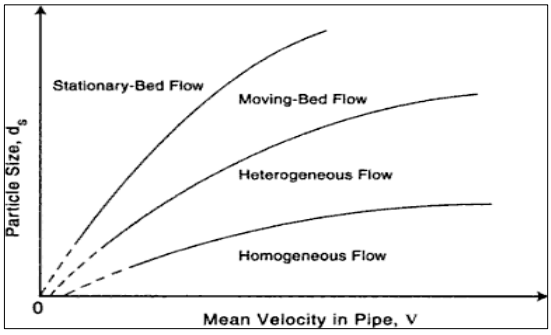

Fig.2 - Sediment flow regime in pipes

Based on the illustration in Figure 2, the settling velocity of a single particle in a fluid is given as follows:

$$w_0^2 = \frac{4gd(\rho_s - \rho_l)}{3C_D\rho_l} \quad (4)$$

is the equation of the terminal velocity of a particle in a fluid, which is used to describe the maximum speed that a particle reaches when the forces acting on it are in equilibrium. Under this condition, the particle's heavy force (F_g) Reduced Fluid Buoyancy Force (F_b) Same as flow inhibitor force (F_D). The equation is obtained by balancing the three forces, where the weight force of the particle is proportional to the volume and density of the particle (ρ_s), Buoyancy force depends on particle volume and fluid density (ρ_l), while the drag force is affected by the drag coefficient (C_D), particle projection area, as well as flow velocity. Physically, this equation shows that the terminal velocity will increase with the increase in particle diameter (d) and the difference in density between particles and fluids ($\rho_s - \rho_l$), while the value greater of the drag coefficient (C_D) or fluid density (ρ_l) will lower the speed of the terminal. In the context of the analysis of sediment movement in a closed pipeline system, this formula is important to determine whether sediment particles will settle or remain carried away in the stream, as well as being the basis for estimating the critical speed required for the pipeline to remain in a self-cleaning condition.

3.5 Proposed Framework

To address the limitations of previous studies and provide a more systematic understanding of sediment dynamics in closed pipe systems, this study proposes a comprehensive analytical framework. The framework integrates laboratory-scale experimental observations with dimensionless parameters such as the Reynolds number, Froude number, and Shields parameter, allowing the results to be normalized and compared across different hydraulic conditions. By combining empirical data with theoretical analysis, the proposed framework not only facilitates the prediction of incipient deposition and critical velocity, but also enhances the applicability of experimental findings to real-world drainage, water supply, and sewage networks. The framework is designed to bridge the gap between laboratory experiments and practical engineering applications, ensuring a robust basis for future optimization of pipeline design and maintenance strategies. Illustration is presented in Figure 3.

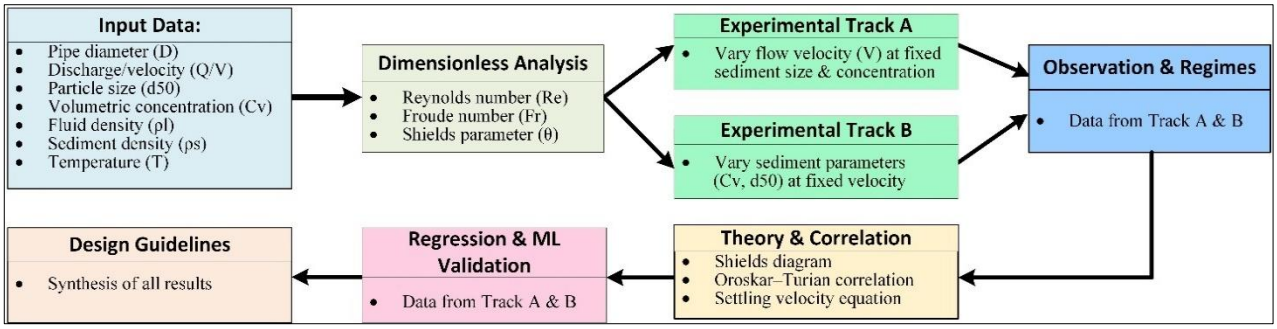

Fig.3 - Proposed framework

The framework includes setting the goals and variables (*D, d50, Cv, Q/V, ρs/ρf, Re*), design pipeline loops & baseline calibration of clean water; run two experimental lines—(A) variation *V* on *d50* and fixed *Cv* to look for critical/self-cleansing velocity and energy penalty (*ΔP*), (*B*) *Cv/d50* variation on selected *V* to see stratifiation, bed-load, and deposition limits. Each step ensures steady flow, sediment mass balance is met, and deposition detection; calculate dimensionless parameters (Shields, Rouse) to map the regime (non-deposition, incipient deposition, deposition/suspension). Consolidate the results into a regime map and curve *Vc(D, d50, Cv)* along with energy needs/flushing strategies; when necessary, validation with models (regression/ML or CFD) for operational predictions. The final output is a stable, sediment-free, and energy-efficient closed pipe operation guideline.

4. Result and Discussion

4.1 Experimental Matrix and Instrumentation

The experiments were conducted to evaluate the relationship between hydraulic pressure and sediment movement in closed pipe flow. The test matrix included variations in pipe diameter (*D* = 25, 50, 75 mm), median particle size (d_{50} = 0.20, 0.35, 1.0 mm), and volumetric sediment concentration (C_v = 0.5%, 1.0%, 2.0%). Flow discharge was adjusted to generate velocities in the range of 0.3–1.5 m/s, allowing the identification of non-deposition (*ND*), incipient deposition (*ID*), and deposition (*D*) regimes.

Hydraulic and sediment parameters were measured using a calibrated electromagnetic flowmeter (accuracy ±1%), differential pressure transducers (0–50 *kPa*, accuracy ±0.25%), and gravimetric analysis of outlet slurry samples. Each operating point was repeated at least three times. Visual

Diterbitkan oleh JPS Publishing
https://journal.water.gov.my

observations of regime transitions were supported by a high-speed camera and LED backlighting, while water temperature was monitored with PT100 sensors to account for viscosity changes. This structured matrix and instrumentation setup ensured reliable identification of critical pressure thresholds and enabled comparison with theoretical models such as the Shields diagram and Oroskar–Turian correlation. The test matrix data is shown in Table 1.

Table 1. Experimental matrix

Factor	Levels	Notes
Pipe diameter (D)	25, 50, 75 mm	Pipe ID and measurement section
Median grain size (d_{50})	0.20, 0.50, 1.00 mm	Prepared by sieving
Sediment concentration (C_v)	0.5%, 1.0%, 2.0%	Volume fraction
Flow velocity (V)	0.3 – 2.5 m/s	Fine steps around critical threshold
Head/Slope	3 levels	For Froude number sensitivity tests
Replications	≥ 3	At each operating point for reliability

An example of calculation based on the data in Table 1 is carried out as follows:
D = 0.050 m
Q = 1.0
L/s = 0.001 m³/s
T = 25 °C Properties of water (±): ρ = 997 kg/m³
μ = 0.00089 Pa·s
$\nu = \mu/\rho = 8.927\times10^{-7}$ m²/s.

1. Average speed

$$V = \frac{4Q}{\pi D^2} = \frac{4(0.001)}{\pi(0.05)^2} = 0.509 \text{ m/s}$$

2. Dimensionless numbers

$$Re = \frac{VD}{\nu} = \frac{0.509 \cdot 0.05}{8.927 \times 10^{-7}} = 2.85 \times 10^4 \text{ (turbulen)}$$
$$Fr = \frac{V}{\sqrt{gD}} = \frac{0.509}{\sqrt{9.81 \cdot 0.05}} = 0.727$$

3. Friction factor (Swamee–Jain, Fine Pipe ε/D = 0.0002)

$$f = \frac{0.25}{\left[\log_{10}\left(\frac{\varepsilon}{3.7D} + \frac{5.74}{Re^{0.9}}\right)\right]^2} \Rightarrow f \approx 0.0243$$

4. Wall shear tension

$$\tau_b = \frac{f\,\rho\,V^2}{8} = \frac{0.0243 \cdot 997 \cdot (0.509)^2}{8} = 0.784 \text{ Pa}$$

5. Parameter Shields (d_{50} = 0.5 mm = 5×10^{-4} m; ρ_s = 2650 kg/m³)

$$\theta = \frac{\tau_b}{(\rho_s - \rho)\,g\,d_{50}} = \frac{0.784}{(2650 - 997) \cdot 9.81 \cdot 5 \times 10^{-4}} = 0.0967$$

The value of θ ≈ 0.097 is generally ≥ θ_c for medium-sized sand.

6. Additional metrics

$$\frac{\Delta P}{L} = \frac{f\,\rho\,V^2}{2D} = \frac{0.0243 \cdot 997 \cdot (0.509)^2}{2 \cdot 0.05} = \mathbf{62.7\ Pa/m}$$

Experiments were carried out 10 times, where the results were shown in Table 2.

Table 2. Regime value testing experiment

Run	Q (L/s)	V (m/s)	Re	Fr	f	τ_β (Pa)	θ (Shields)	Regime
1	1.062	0.541	3.03×10^4	0.77	0.0239	0.872	0.108	ND
2	1.466	0.747	4.18×10^4	1.07	0.0223	1.552	0.191	ND
3	1.312	0.668	3.74×10^4	0.95	0.0229	1.272	0.157	ND
4	1.219	0.621	3.48×10^4	0.89	0.0232	1.116	0.138	ND
5	0.909	0.463	2.59×10^4	0.66	0.0248	0.662	0.082	ND
6	0.909	0.463	2.59×10^4	0.66	0.0248	0.662	0.082	ND
7	0.841	0.428	2.40×10^4	0.61	0.0252	0.577	0.071	ND
8	1.406	0.716	4.01×10^4	1.02	0.0225	1.440	0.178	ND
9	1.221	0.622	3.48×10^4	0.89	0.0232	1.119	0.138	ND
10	1.296	0.660	3.70×10^4	0.94	0.0229	1.245	0.154	ND

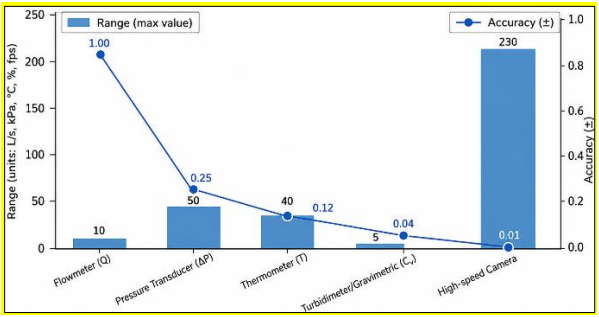

Fig.4 - Result of Instrumentation used for hydraulic and sediment measurements

Diterbitkan oleh JPS Publishing
https://journal.water.gov.my

Based on Figure 4, it is shown that the Shields' results for all scenarios showed value of θ > 0.06, meaning that the sediment was in a Non-Deposition (*ND*) state (Ganat, 2024). Furthermore, Figure 4 measurement range and accuracy of instruments used in the experimental setup. The flowmeter, pressure transducer, thermometer, turbidimeter/gravimetric method, and high-speed camera were each calibrated within their specified ranges to ensure precise monitoring of discharge (Q), pressure drop (ΔP), temperature (T), sediment concentration (C_v), and visual flow regimes. The combination of quantitative sensors and visual observation minimized uncertainty and provided robust data for subsequent dimensionless analysis and regime classification (Matsumoto et al., 2025).

4.2 Pressure Drop and Critical Velocity

To evaluate the hydraulic performance under varying sediment and flow conditions, the pressure drop per unit length (ΔP/L) was plotted against the mean flow velocity (V). This analysis provides insights into the energy penalty associated with increasing velocity and helps identify the self-cleansing threshold where non-deposition (ND) conditions are sustained. The observed flow regimes were classified as deposition (D), incipient deposition (ID), and non-deposition (ND) based on visual observations and sediment sampling, and these categories are annotated in the graph for clarity, as shown in Figure 5.

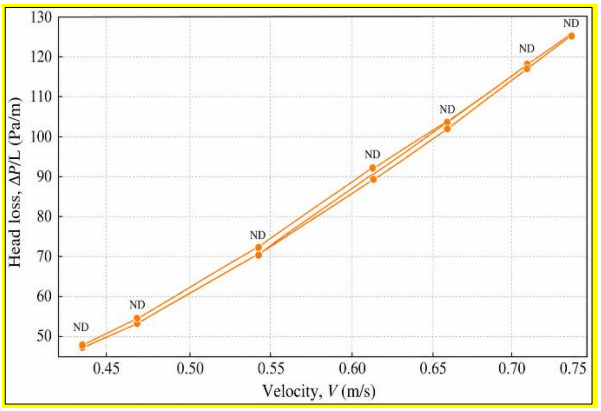

Fig.5 - The relationship of head loss per unit length to the flow rate

4.3 Regime Map and Comparison with Theoretical Models

To analyse the velocity–pressure relationship, the experimental data were expressed in terms of dimensionless parameters to facilitate comparison with theoretical predictions. By plotting the Shields parameter (θ) against the Reynolds number (Re), a regime map was constructed to visualize the transition boundaries between deposition, incipient deposition, and non-deposition. The distribution of experimental points across these regimes is presented in Figure 6.

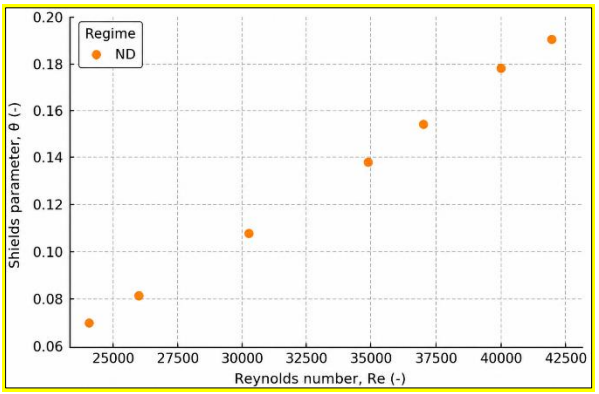

Fig.6 - Distribution of experimental points across these regimes

To generalize the findings, the experimental data were further analyzed using dimensionless parameters. Figure 6 shows the regime map constructed by plotting the Shields parameter (θ) against the Reynolds number (Re). The data distribution highlights clear boundaries between the deposition, incipient deposition, and non-deposition regimes, providing a practical tool for identifying self-cleansing conditions in closed pipe systems.

When compared with the Shields diagram, the critical θ values observed in this study are generally higher than the classical range of 0.03–0.06 reported for open-channel flows. This difference can be attributed to the confined geometry of closed pipes and the turbulent boundary layer effects, which elevate the shear stress required to initiate sediment motion. Likewise, the Oroskar–Turian correlation, widely applied for slurry transport pipelines, tends to underestimate the experimental Vc values. The discrepancy arises from particle distribution effects, pipe diameter scaling, and the relatively low sediment concentrations employed in the experiments.

Despite these differences, both theoretical and empirical comparisons confirm that the onset of ND conditions is strongly influenced not only by velocity but also by the interplay of hydraulic pressure, sediment properties, and geometric confinement. These results support the adoption of a pressure-based criterion for designing self-cleansing closed pipe systems.

4. Conclusion

This study experimentally evaluated hydraulic pressure thresholds for sediment movement in closed pipe systems. The results show that pressure-based analysis provides a reliable criterion for identifying self-cleansing conditions. The ΔP/L–V relationship confirmed that the critical velocity (Vc) corresponds to the minimum velocity sustaining non-deposition (ND) with acceptable energy efficiency, while the θ–Re regime map effectively classified deposition (D), incipient deposition (ID), and ND boundaries. Comparisons with theoretical models indicated that experimental θ values were higher than classical Shields predictions, and Oroskar–Turian correlations tended to underestimate Vc, highlighting the influence of pipe confinement and turbulence.

Implications. These findings advance sediment transport theory and offer practical guidance for designing energy-efficient drainage, water supply, and sewage pipelines using pressure-based criteria.

Limitations. The study was constrained to laboratory-scale diameters, steady-state flows, and uniform sediments, limiting direct applicability to field conditions. Future

Diterbitkan oleh JPS Publishing
https://journal.water.gov.my

research should explore larger scales, mixed sediments, and unsteady flows, integrating CFD and machine learning for broader predictive capability.

References

[1] Alkahtani, B. S. T., Agrawal, K., Kumar, S., & Alzaid, S. S. (2023). Bernoulli polynomial based wavelets method for solving chaotic behaviour of financial model. *Results in Physics*, *53*, 107011. https://doi.org/https://doi.org/10.1016/j.rinp.2023.107011

[2] Aung, Z. Y., Vo, D., Suttakul, P., Atroshchenko, E., Bui, T. Q., & Rungamornrat, J. (2024). Peridynamic formulations for planar arbitrarily curved beams with Euler-Bernoulli beam model. *Thin-Walled Structures*, *204*, 112278. https://doi.org/https://doi.org/10.1016/j.tws.2024.112278

[3] Babar, H., Wu, H., Eltaweel, M., & Zhang, W. (2025). Performance evaluation of nanofluid-enhanced biomimetic liquid-cooled heat sinks for efficient thermal management applications. *International Journal of Heat and Mass Transfer*, *252*, 127498. https://doi.org/10.1016/j.ijheatmasstransfer.2025.127498

[4] Casini, M. (2022). Chapter 2 - Holistic building design approach. In M. B. T.-C. 4. . Casini (Ed.), *Woodhead Publishing Series in Civil and Structural Engineering* (pp. 61–149). Woodhead Publishing. https://doi.org/https://doi.org/10.1016/B978-0-12-821797-9.00001-5

[5] Chen, D., Zheng, S., Zhang, J., Li, H., Nie, B., Lian, B., & Wang, D. (2025). An isotope tracer experiment for simulating tritiated water vapor transfer and accumulation at the air-water interface. *Journal of Cleaner Production*, *513*, 145737. https://doi.org/10.1016/j.jclepro.2025.145737

[6] Coker, A. K. (2024). Pressure-Relieving Devices and Process Safety Incidents. In A. K. B. T.-L. s A. P. D. for C. and P. P. I. P. S. I. (Fifth E. Coker (Ed.), *Ludwig' s Applied Process Design for Chemical and Petrochemical Plants Incorporating Process Safety Incidents* (pp. 1585–1956). Elsevier. https://doi.org/10.1016/B978-0-443-30114-8.00009-2

[7] Ding, S., Shen, X., & Cai, Z. (2024). Data-driven multi-step solar photovoltaic predictions with limited and uncertain information: Insights from a collaboratively-optimized nonlinear grey Bernoulli model. *Expert Systems with Applications*, *258*, 125170. https://doi.org/https://doi.org/10.1016/j.eswa.2024.125170

[8] Ganat, T. (2024). Experimental investigation of viscous oil–water–sand flow in horizontal pipes: Flow patterns and pressure gradient. *Petroleum*, *10*(2), 275–293. https://doi.org/10.1016/j.petlm.2023.09.005

[9] García-Grimaldo, C., & Campos-Cantón, E. (2023). Exploring a family of Bernoulli-like shift chaotic maps and its amplitude control. *Chaos, Solitons & Fractals*, *175*, 113951. https://doi.org/https://doi.org/10.1016/j.chaos.2023.113951

[10] Gong, Y., & Wang, J. (2024). Turbulence model adaptability at critical Reynolds numbers and applications in wake control via fairings. *Applied Ocean Research*, *153*, 104263. https://doi.org/https://doi.org/10.1016/j.apor.2024.104263

[11] Gooran, S., Shabanian, S. R., & Ghorbani, M. (2025). Experimental study on critical heat flux enhancement and stability of nanofluid containing copper oxide and polypyrrole nanocomposite. *Journal of Molecular Liquids*, *426*, 127494. https://doi.org/10.1016/j.molliq.2025.127494

[12] Jang, D. S., Ham, S. H., Shin, H. H., & Kim, Y. (2024). Thermal performance improvement of a radial pulsating heat pipe with diverging channels by adopting Tesla valves at various heat fluxes. *Applied Thermal Engineering*, *237*, 121799. https://doi.org/https://doi.org/10.1016/j.applthermaleng.2023.121799

[13] Kargar, K., Safari, M. J. S., & Khosravi, K. (2021). Weighted instances handler wrapper and rotation forest-based hybrid algorithms for sediment transport modeling. *Journal of Hydrology*, *598*(May), 126452. https://doi.org/10.1016/j.jhydrol.2021.126452

[14] Li, Z. P., Peng, Z., Kiani-Oshtorjani, M., Liu, M., Zhang, F., Chen, Y., & Zhu, Y. (2024). A generalization of the Exner law for sediment nonlocal transport at bedform scale. *Journal of Hydrology*, *645*, 132236. https://doi.org/10.1016/j.jhydrol.2024.132236

[15] Lienhard, J., Nelson, K. A., & Schuh, C. A. (2022). Tin and zinc microparticle impacts above the critical adhesion velocity. *Surface and Coatings Technology*, *432*, 128053. https://doi.org/10.1016/j.surfcoat.2021.128053

[16] Liu, J., Cao, Z., & Li, X. (2022). Coupled modelling of flow and non-capacity sediment transport in sewer flushing channel. *Water Research*, *219*, 118557. https://doi.org/10.1016/j.watres.2022.118557

[17] Luo, Y., Xiao, H., Liu, X., Qin, Y., Wu, Z., & Zheng, T. (2023). Multiphase nanoconfined fluid flow mechanisms in nanopores, insights derived from molecular dynamics. *Chemical Engineering Journal*, *474*, 145946. https://doi.org/https://doi.org/10.1016/j.cej.2023.145946

[18] Matsumoto, S., Tum, S., Ogino, T., Nishikata, M., Yasutaka, T., Oguri, T., & Shintani, T. (2025). Identification of inflow sources and pathways to a waste rock dump located in a former river channel in a mountainous abandoned mine of Japan: A case study 60 years post-construction. *Journal of Hydrology: Regional Studies*, *61*. https://doi.org/10.1016/j.ejrh.2025.102645

[19] Monokrousos, N., Könözsy, L., Pachidis, V., Sozio, E., & Rossi, F. (2024). A numerical approach to overcome the very-low Reynolds number limitation of the artificial compressibility for incompressible flows. *Heliyon*, *10*(21), e39587. https://doi.org/https://doi.org/10.1016/j.heliyon.2024.e39587

[20] Montes, C., Berardi, L., Kapelan, Z., & Saldarriaga, J. (2020). Predicting bedload sediment transport of non-cohesive material in sewer pipes using evolutionary polynomial regression–multi-objective genetic algorithm strategy. *Urban Water Journal*, *17*(2), 154–162. https://doi.org/10.1080/1573062X.2020.1748210

[21] Naves, J., Anta, J., Suárez, J., & Puertas, J. (2020). Hydraulic, wash-off and sediment transport experiments in a full-scale urban drainage physical model. *Scientific Data*, *7*(1), 1–13. https://doi.org/10.1038/s41597-020-0384-z

[22] Orang, M., & Pouranfard, A. (2022). Experimental, comparative and statistical study of heat transfer and drag reduction of Water/Polyisobutylene/nanoSiO2 poly-nanofluid through a horizontal pipe. *Chemical Engineering Research and Design*, *183*, 466–477. https://doi.org/10.1016/j.cherd.2022.05.052

[23] Safari, M. J. S., & Rahimzadeh Arashloo, S. (2023). Robust low-rank learning multi-output regression for incipient sediment motion in sewer pipes. *International Journal of Sediment Research*, *38*(6), 859–870. https://doi.org/10.1016/j.ijsrc.2023.08.004

[24] Sha, F., Xu, J., Gu, S., Dong, Y., & Xiao, W. (2025). A review on fluid-sediment and foundation-sediment coupling mechanisms and anti-scour countermeasures. *Marine Structures*, *103*. https://doi.org/10.1016/j.marstruc.2025.103843

[25] Taiwo, R., Zayed, T., Elshaboury, N., Alfalah, G., & Abdelkader, E. M. (2025). Promoting sustainable water distribution networks: Modeling of water pipe failure factors and modes. *Cleaner Engineering and Technology*, *26*, 100969. https://doi.org/10.1016/j.clet.2025.100969

[26] Thorn, C., Paula, F. S., Brennan, F., & Abram, F. (2025). Cattle slurry application increases soil ecosystem resistance to flooding. *Applied Soil Ecology*, *214*. https://doi.org/10.1016/j.apsoil.2025.106323

[27] Wang, Q., Yu, C., Li, T., Wang, J., Liu, Y., Shi, Y., Song, Y., Chang, H., Peng, W., & Niu, Y. (2024). Enhancing the performance of PVT-TEG power generation systems by heat pipes and Fe3O4 nanofluids. *Energy Conversion and Management*, *319*, 118938. https://doi.org/10.1016/j.enconman.2024.118938

[28] Yao, D., Sun, X., Qu, J., Yang, H., Tao, L., & Hu, Q. (2025). Application of drift flux model in solid-liquid flow in horizontal wellbores. *Geoenergy Science and Engineering*, *253*, 213964. https://doi.org/10.1016/j.geoen.2025.213964

[29] Zhang, S., Ren, H., Zhang, D., Wang, S., Zhang, H., Luo, R., & Feng, Y. (2023). Air gap fluid flow characteristics of high-power water-cooled submersible motors. *Desalination and Water Treatment*, *314*, 330–338.https://doi.org/https://doi.org/10.5004/dwt.2023.30038